Published in Proceedings of the European Numerical Mathematics and Advanced Applications Conference 2019, 30.09-04.10, Egmond aan Zee, The Netherlands, "Numerical Mathematics and Advanced Applications ENUMATH 2019", Springer 2021, ISBN 978-3-030-55873-4 which should be cited to refer to this work.

A second order time integration method for the approximation of a parabolic 2D Monge-Ampère equation

Alexandre Caboussat and Dimitrios Gourzoulidis

Abstract Parabolic fully nonlinear equations may be found in various applications, for instance in optimal portfolio management strategy. A numerical method for the approximation of a canonical parabolic Monge-Ampère equation is investigated in this work. A second order semi-implicit time-stepping method is presented, coupled to safeguarded Newton iterations A low order finite element method is used for space discretization. Numerical experiments exhibit appropriate convergence orders and a robust behavior.

1 Introduction

Fully nonlinear equations, and among them the elliptic Monge-Ampère equation, have raised a lot of interest from the theoretical and numerical communities [1, 7, 9, 10], and also from the authors [4, 6]. We focus here on a time-evolutive, parabolic, Monge-Ampère equation that has raised much less attention from a computational perspective. Some known applications of interest arise, e.g., in finance [12], or in mesh adaptation techniques [2, 3]. Numerical results for parabolic fully nonlinear equations, including the equation that we study here, are given, e.g., in [8].

The purpose of this work is to introduce a second-order semi-implicit numerical scheme for the approximation of the time-evolutive Monge-Ampère equation. It extends the Newton-based approaches in [1, 10] to the non-stationary case by means of a midpoint time-stepping algorithm. Continuous, low order, finite elements are

Alexandre Caboussat
Geneva School of Business Administration, University of Applied Sciences and Arts Western Switzerland (HES-SO), e-mail: alexandre.caboussat@hesge.ch

Dimitrios Gourzoulidis
Geneva School of Business Administration, University of Applied Sciences and Arts Western Switzerland (HES-SO), and Institute of Mathematics, Ecole Polytechnique Fédérale de Lausanne, e-mail: dimitrios.gourzoulidis@hesge.ch, dimitrios.gourzoulidis@epfl.ch

used for the space discretization. Numerical validation is achieved with simple examples, and appropriate convergence results are obtained from a computational perspective.

2 Model problem

Let Ω be a smooth bounded convex domain of $\mathbb{R}^2$, and $T > 0$ a fixed time horizon. We consider a time evolutive two-dimensional Monge-Ampère equation, with Dirichlet boundary conditions, which reads as follows: find $u : \Omega \times (0,T) \to \mathbb{R}$ satisfying

$$\begin{cases} \dfrac{\partial u}{\partial t} - \det \mathbf{D}^2 u = f & \text{in } \Omega \times (0,T), \\ u = g & \text{in } \partial\Omega \times (0,T), \\ u(0) = u_0 & \text{in } \Omega. \end{cases} \tag{1}$$

Here $f = f(\mathbf{x},t)$, $g = g(\mathbf{x},t)$ and $u_0 = u_0(\mathbf{x})$ are given functions with the required regularity, and $\mathbf{D}^2 u (:= \mathbf{D}^2_{\mathbf{x}} u)$ is the Hessian of the unknown function u (with respect to the space variable $\mathbf{x}$), defined by $\mathbf{D}^2 u = (D^2_{ij} u)_{1 \le i,j \le 2}$, and $D^2_{ij} u = \dfrac{\partial^2 u}{\partial x_i \partial x_j}$.

We assume in the sequel that u_0 is convex, in order to favor the regularity of a smooth transient. A constraint on the time step may have to be enforced to make sure that the numerical solution remains convex at all times. Numerical results will show that the right-hand side f may change sign, as long as the numerical solution remains convex and the operator in the parabolic Monge-Ampère equation remains coercive. Following [9], the Monge-Ampère operator can be rewritten under a divergence form, namely

$$\det \mathbf{D}^2 u = \frac{1}{2} \nabla \cdot \left(\mathrm{cof}(\mathbf{D}^2 u) \nabla u \right).$$

The differential operator of (1) can thus be written as

$$\frac{\partial u}{\partial t} - \frac{1}{2} \nabla \cdot \left(\mathrm{cof}(\mathbf{D}^2 u) \nabla u \right) = f \quad \text{in } \Omega \times (0,T), \tag{2}$$

meaning that (1) can be interpreted as a, strongly nonlinear, parabolic equation reminiscent of a nonlinear heat equation. When looking for a convex solution, if the nonlinearity $\mathrm{cof}(\mathbf{D}^2 u)$ remains positive definite, then the operator is well-posed. The challenge becomes thus to capture convex solutions, and to derive numerical methods that take into account accurately the strongly nonlinear diffusion and guarantee the coercivity of the diffusion operator at all times.

Remark 1 In [9], an alternative formulation is considered, which consists in augmenting the differential equation into a differential system. This approach has proved to be very efficient in capturing a stationary solution. However, numerical experiments have shown that it is not efficient to approximate the whole transient trajectory of the evolutive problem.

In the sequel, we thus propose a second-order numerical method for the numerical approximation of the solution of (1), which relies on an implicit time-stepping scheme and a Newton's method.

3 Numerical algorithm

Let $\Delta t > 0$ be a constant given time step, $t^n = n\Delta t$, $n = 1, 2, \ldots$, to define the approximations $u^n \simeq u(t^n)$. The numerical algorithm proposed hereafter relies on a discretization of the formulation (1) In order to handle the stiff behavior of the Monge-Ampère equation, a semi-implicit time discretization of (1) is considered. In this case, we advocate a *midpoint rule* and, u^n being known, we look for the next time step approximation u^{n+1} satisfying

$$\frac{u^{n+1} - u^n}{\Delta t} - \det\left(\mathbf{D}^2 u^{n+1/2}\right) = f^{n+1/2} \quad n = 0, 1, \ldots, \tag{3}$$

where $u^{n+1/2} := \dfrac{u^{n+1} + u^n}{2}$ and $f^{n+1/2} := f\left(\dfrac{t^{n+1} + t^n}{2}\right)$. Then (3) can be written as

$$u^{n+1/2} - \frac{1}{2}\Delta t \det \mathbf{D}^2 u^{n+1/2} = u^n + \frac{1}{2}\Delta t f^{n+1/2}, \tag{4}$$

and

$$u^{n+1} = 2u^{n+1/2} - u^n. \tag{5}$$

Let us define $b^n := u^n + \frac{1}{2}\Delta t f^{n+1/2}$. Relationship (4) is rewritten at each time step as

$$F(u^{n+1/2}) := u^{n+1/2} - \frac{\Delta t}{2}\det(\mathbf{D}^2 u^{n+1/2}) - b^n = 0.$$

This nonlinear problem is solved with a safeguarded Newton method at each time step. For the ease of notation, we denote $u^{n+1/2}$ by v. Starting from the initial guess $v^0 = u^n$, the increments δv^k of the Newton method are obtained by solving

$$DF(v^k)\delta v^k = -F(v^k), \quad k = 0, 1, 2, \ldots, \tag{6}$$

then, the next iterate is given by $v^{k+1} = v^k + \delta v^k$, until some stopping criterion is satisfied at step M, and set $u^{n+1/2} := v^M$. At the end of the Newton loop, the approximation of the solution at the next time step is given by (5). In order to write the variational formulation corresponding to (6) we use the following identity which holds for 2×2 symmetric matrices (see, e.g., [1]):

$$\det \mathbf{D}^2(a + b) = \det(\mathbf{D}^2 a) + \det(\mathbf{D}^2 b) + \mathrm{tr}(A^* \mathbf{D}^2 b), \tag{7}$$

where $A^* = \mathrm{cof}(\mathbf{D}^2 a) = \det(\mathbf{D}^2 a)(\mathbf{D}^2 a)^{-1}$. This yields

$$\mathrm{tr}(A^* \mathbf{D}^2 b) = \mathrm{cof}(\mathbf{D}^2 a) : \mathbf{D}^2 b = \nabla \cdot (\mathrm{cof}(\mathbf{D}^2 a)\nabla b),$$

where $\mathbf{A} : \mathbf{B} := \mathrm{tr}(\mathbf{A}^T\mathbf{B})$ is the Frobenius inner product for $\mathbf{A},\ \mathbf{B} \in \mathbb{R}^{2\times 2}$. Equation (7) becomes,

$$\det \mathbf{D}^2(a+b) = \det(\mathbf{D}^2 a) + \nabla \cdot (\mathrm{cof}(\mathbf{D}^2 a)\nabla b) + \det(\mathbf{D}^2 b). \tag{8}$$

We thus have, for $s \in \mathbb{R}$,

$$F(v^k + s\delta v) = v^k + s\delta v - \frac{\Delta t}{2}\left(\det(\mathbf{D}^2 v^k) + \nabla \cdot (\mathrm{cof}(\mathbf{D}^2 v^k) s\nabla\delta v) + s^2 \det(\mathbf{D}^2\delta v)\right) - b^n.$$

We thus compute $DF(v^k)$ as follows:

$$DF(v^k)\delta v = \lim_{s\to 0} \frac{F(v^k + s\delta v) - F(v^k)}{s} = \delta v - \frac{\Delta t}{2}\nabla \cdot \left(\mathrm{cof}(\mathbf{D}^2 v^k)\nabla\delta v\right). \tag{9}$$

In order to incorporate (9) in the variational formulation corresponding to (6), let us define $V_g = \left\{w \in H^1(\Omega) :\ w|_{\partial\Omega} = g\right\}$, and $V_0 = H_0^1(\Omega)$. Using (9), the variational formulation corresponding to the Newton system (6) can be explicited into : find $\delta v^k \in V_0$, for $k = 0, 1, 2, \ldots$, such that

$$\begin{aligned}\int_\Omega \delta v^k w d\mathbf{x} + \frac{\Delta t}{2}\int_\Omega \mathrm{cof}(\mathbf{D}^2 v^k)\nabla(\delta v^k)\cdot\nabla w d\mathbf{x} = \\ -\int_\Omega \left(v^k - \frac{\Delta t}{2}\det(\mathbf{D}^2 v^k) - b^n\right) w d\mathbf{x},\end{aligned} \tag{10}$$

for all $w \in V_0$. This Newton's variational problem is coupled with a safeguarding strategy (Armijo's rule) when needed. In addition, the method guarantees that the matrix $\mathrm{cof}(\mathbf{D}^2 v^k)$ remains positive definite. This procedure is achieved by computing the SVD of this matrix, and truncating its negative eigenvalues to zero.

4 Finite Element Discretization

In order to avoid the construction of finite element sub-spaces of $H^2(\Omega)$ and to handle arbitrary shaped domains, we consider a mixed low order finite element method for the approximation of (10) see, e.g., [4, 6]. Let us thus denote by $\mathcal{T}_h$ a regular finite element discretization of $\Omega \subset \mathbb{R}^2$ in triangles. From $\mathcal{T}_h$, we approximate the spaces $L^2(\Omega)$, $H^1(\Omega)$ and $H^2(\Omega)$, respectively $H_0^1(\Omega)$ and $H^2(\Omega) \cap H_0^1(\Omega)$, by the finite dimensional space V_h, respectively V_{0h}, defined by:

$$V_h = \left\{v \in C^0\left(\overline{\Omega}\right),\ v|_K \in \mathbb{P}_1,\ \forall K \in \mathcal{T}_h\right\}, \quad V_{0,h} = V_h \cap H_0^1(\Omega), \tag{11}$$

with $\mathbb{P}_1$ the space of the two-variables polynomials of degree one. Moreover, let us define $V_{g,h} = \left\{v \in C^0\left(\overline{\Omega}\right),\ v|_K \in \mathbb{P}_1,\ \forall K \in \mathcal{T}_h,\ v|_{\partial\Omega} = g\right\}$. As in [6], for a function

φ being given in $H^1(\Omega)$, we approximate the differential operators D^2_{ij} by D^2_{hij}, for $1 \le i, j \le 2$, defined by $D^2_{hij}(\varphi) \in V_{0h}$ and

$$\int_\Omega D^2_{hij}(\varphi) v d\mathbf{x} = -\frac{1}{2}\int_\Omega \left[\frac{\partial \varphi}{\partial x_i}\frac{\partial v}{\partial x_j} + \frac{\partial \varphi}{\partial x_j}\frac{\partial v}{\partial x_i}\right] d\mathbf{x}, \ \forall v \in V_{0h}. \tag{12}$$

As emphasized in [11], the a priori estimates for the error on the second derivatives of the solution φ are, in general, $O(1)$ in the L^2-norm when using piecewise linear mixed finite elements. Therefore the convergence properties of the solution method depend strongly on the type of triangulations one employs. To cure the non-convergence properties associated with the approximations of $D^2_{hij}(\varphi)$, we use a regularization procedure as in [6], and we replace (12) by: find $D^2_{hij}(\varphi) \in V_{0h}$, $1 \le i, j \le 2$, such that

$$\int_\Omega D^2_{hij}(\varphi) v d\mathbf{x} + C \sum_{K \in \mathcal{T}_h} |K| \int_K \nabla D^2_{hij}(\varphi) \cdot \nabla v d\mathbf{x} = -\frac{1}{2}\int_\Omega \left[\frac{\partial \varphi}{\partial x_i}\frac{\partial v}{\partial x_j} + \frac{\partial \varphi}{\partial x_j}\frac{\partial v}{\partial x_i}\right] d\mathbf{x},$$

where $C \ge 0$ and $|K| = \text{meas}(K)$, Set u^0_h be an approximation of u^0 in $V_{g,h}$. At each time step, the numerical approximation of (10) is computed as follows: let $v^0_h := u^n_h$ at each time iteration; then, for $k = 0, 1, 2, \ldots$, we search for $\delta v^k_h \in V_{0,h}$ such that:

$$\int_{\Omega_h} \delta v^k_h w_h d\mathbf{x} + \frac{\Delta t}{2}\int_{\Omega_h} \text{cof}(\mathbf{D}^2 v^k_h)\nabla(\delta v^k_h) \cdot \nabla w_h d\mathbf{x} = -\int_\Omega \left(v^k_h - \frac{\Delta t}{2}\det(\mathbf{D}^2 v^k_h) - b^n_h\right) w_h d\mathbf{x}, \tag{13}$$

for all $w_h \in V_{0,h}$. Then we set $v^{k+1}_h := v^k_h + \delta v^k_h$; when some stopping criterion is satisfied at step M, we set $u^{n+1/2}_h := v^M_h$. To progress to the next time step, we compute $u^{n+1}_h = 2u^{n+1/2}_h - u^n_h$.

5 Numerical Experiments

Numerical results are presented to validate the method for convex solutions. In the following examples, $\Omega = (0, 1)^2$ and $T = 1$. Both a triangular structured asymmetric mesh and an unstructured isotropic mesh are used. The mesh size h and the time step Δt vary together. The stopping criterion for the Newton method is $||v^{k+1}_h - v^k_h||_{L_2(\Omega)} \le 10^{-12}$, with a maximal number of 200 Newton iterations. The Newton method

typically needs $9-12$ iterations to converge, depending on the mesh size and the time step. The parameter C is set to 1 (unless specified otherwise). The convergence of the error $e = u - u_h$ is quantified by the following quantities

$$||e||_{L^2(L^2)} := \int_0^T \|u - u_h\|_{L^2}\, dt, \quad ||e||_{L^2(H^1)} := \int_0^T \|\nabla u - \nabla u_h\|_{L^2}\, dt,$$

In the tables below, those norms are approximated using the trapezoidal rule in time, and quadrature formulas in space (see [5]).

5.1 A polynomial example

Let us consider $T = 1$, and the exact solution:

$$u(x, y, t) = 0.5\,(0.5 + t)\,(x^2 + 5y^2), \qquad (x, y) \in \Omega, \quad t \in (0, T)\,. \tag{14}$$

This function is the solution of (1) with the data $f(x, y, t) := 0.5\left(x^2 + 5y^2\right) - 5\,(0.5 + t)^2$, $g(x, y, t) := 0.5\,(0.5 + t)\,(x^2 + 5y^2)$, and $u_0(x, y) := 0.25(x^2 + 5y^2)$. The solution (14) is convex for all $t \in (0, T)$. Note that the eigenvalues of the Hessian $\mathbf{D}^2 u$ are $\lambda_1 = (0.5 + t)^2$ and $\lambda_2 = 5\,(0.5 + t)^2$, and are both positive for all $t \in (0, T)$. Figure 1 illustrates $u_{0,h}(x, y)$ (left) and $u_h(x, y, T)$ (right), while Table 1 shows that the solution method exhibits appropriate convergence orders (for the discrete version of the norms $||u - u_h||_{L^2(0,T;H^1(\Omega))}$ and $||u - u_h||_{L^2(0,T;L^2(\Omega))}$).

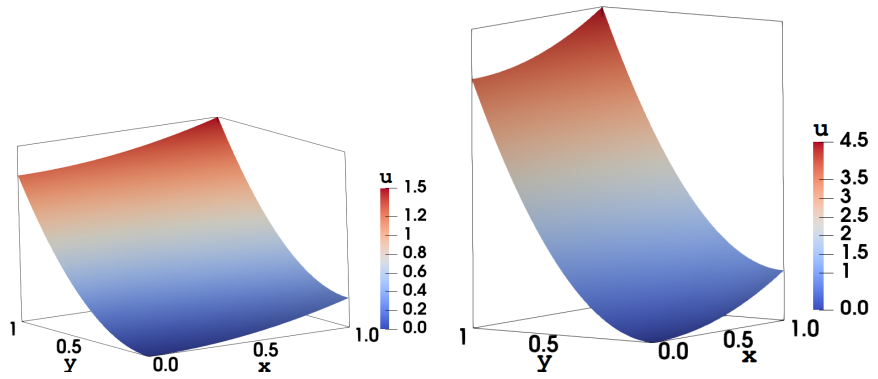

Fig. 1 A polynomial example corresponding to the exact solution (14). Numerical approximation of the solution for $h = 1/80$ and $\Delta t = 0.25 \cdot 10^{-3}$. Left: initial condition at time $t = 0$. Right: final solution at time $t = 1$.

Table 1 A polynomial example. Estimated errors of $u - u_h$ in corresponding norms, and related convergence orders for various h and Δt. Left: structured meshes (with $C = 0$), right: unstructured meshes.

h	Δt	$\|\|e\|\|_{L^2(L^2)}$		$\|\|e\|\|_{L^2(H^1)}$	
1/20	1.00e-03	1.55e-03	-	7.37e-02	-
1/40	0.50e-03	3.81e-04	2.02	3.68e-02	1.00
1/80	0.25e-03	9.01e-05	2.08	1.84e-02	1.00
1/160	0.125e-03	1.99e-05	2.17	9.20e-03	1.00

h	Δt	$\|\|e\|\|_{L^2(L^2)}$		$\|\|e\|\|_{L^2(H^1)}$	
0.062	2.00e-03	2.10e-02	-	3.19e-01	-
0.031	1.00e-03	7.28e-03	1.52	1.51e-01	1.07
0.015	0.50e-03	1.90e-03	1.93	6.14e-02	1.29
0.010	0.33e-03	8.29e-04	2.04	3.49e-02	1.39

5.2 An exponential example

Let us consider $T = 1$, and the exact solution

$$u(x, y, t) = e^{-t} e^{\frac{1}{2}(x^2+y^2)}, \qquad (x, y) \in \Omega, \quad t \in (0, T)\,. \tag{15}$$

This function is the solution of (1) with the data

$$f(x, y, t) := -e^{-t} e^{\frac{1}{2}(x^2+y^2)} \left(1 + e^{-t} \left(x^2 + y^2 + 1\right) e^{\frac{1}{2}(x^2+y^2)}\right),$$

together with $g(x, y, t) := e^{-t} e^{\frac{1}{2}(x^2+y^2)}$, and $u_0(x, y) := e^{\frac{1}{2}(x^2+y^2)}$. The solution (15) is convex for all time $t \in (0, T)$, since the eigenvalues of $\mathbf{D}^2 u$ are $\lambda_1 = e^{-t} e^{\frac{1}{2}(x^2+y^2)}$, and $\lambda_2 = e^{-t} e^{\frac{1}{2}(x^2+y^2)} \left(x^2 + y^2 + 1\right)$, which are both positive for all times $t \in (0, T)$. Figure 2 illustrates $u_{0,h}(x, y)$ (left) and $u_h(x, y, T)$ (right), while Table 2 shows that the solution method exhibits nearly optimal convergence orders (for structured and unstructured mesh we have $O(h)$ and $O(h^{1.5})$ for the discrete version of the norm $||e||_{L^2(H^1)}$ and $O(h^{1.8})$ and $O(h^2)$ for $||e||_{L^2(L^2)}$, respectively)

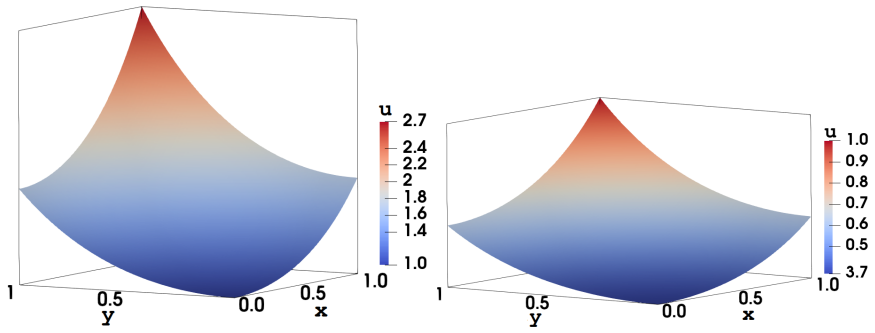

Fig. 2 Exponential example corresponding to the exact solution (15). Numerical approximation of the solution for $h = 1/80$ and $\Delta t = 0.25 \cdot 10^{-3}$. Left: initial condition at time $t = 0$. Right: the final solution at time $t = 1$.

Table 2 Exponential example. Estimated errors of $u - u_h$ in corresponding norms, and related convergence orders for various h and Δt. Left: structured meshes (with $C = 0$ when $h \geq 1/80$, and $C = 0.1$ when $h = 1/160$), right: unstructured meshes.

h	Δt	$\|\|e\|\|_{L^2(L^2)}$		$\|\|e\|\|_{L^2(H^1)}$	
1/20	1.00e-03	8.96e-04	-	3.58e-02	-
1/40	0.50e-03	2.40e-04	1.90	1.79e-02	1.00
1/80	0.25e-03	6.69e-05	1.80	8.96e-03	0.99
1/160	0.125e-03	9.97e-06	2.74	4.44e-03	1.01

h	Δt	$\|\|e\|\|_{L^2(L^2)}$		$\|\|e\|\|_{L^2(H^1)}$	
0.062	2.00e-03	1.49e-02	-	2.02e-01	-
0.031	1.00e-03	5.31e-03	1.48	8.93e-02	1.17
0.015	0.50e-03	1.25e-03	2.08	3.27e-02	1.44
0.010	0.33e-03	5.26e-04	2.13	1.81e-02	1.45

Acknowledgments

This work was partially supported by the Swiss National Science Foundation (Grant #165785). The authors thank Prof. Marco Picasso (EPFL), and Prof. R. Glowinski (Univ. of Houston/Hong Kong Baptist Univ.) for helpful comments and discussions.

References

1. S. C. Brenner and M. Neilan. Finite element approximations of the three dimensional Monge-Ampère equation. *ESAIM: M2AN*, 46(5):979–1001, 2012.
2. C. J. Budd, M. J. P. Cullen, and E. J. Walsh. Monge-Ampère based moving mesh methods for numerical weather prediction, with applications to the Eady problem. *J. Comput. Phys.*, 236:247–270, 2013.
3. C.J. Budd and J. F. Williams. Moving mesh generation using the parabolic Monge-Ampère equation. *SIAM J. Sci. Comput.*, 31:3438–3465, 2009.
4. A. Caboussat, R. Glowinski, and D. Gourzoulidis. A least-squares/relaxation method for the numerical solution of the three-dimensional elliptic Monge-Ampère equation. *J. Sci. Comp.*, 77:53–78, 2018.
5. A. Caboussat, R. Glowinski, D. Gourzoulidis, and M. Picasso. Numerical approximation of orthogonal maps. *SIAM J. Sci. Comput.*, 41:B1341–B1367, 2019.
6. A. Caboussat, R. Glowinski, and D. C. Sorensen. A least-squares method for the numerical solution of the Dirichlet problem for the elliptic Monge-Ampère equation in dimension two. *ESAIM: Control, Optimization and Calculus of Variations*, 19(3):780–810, 2013.
7. X. Feng, R. Glowinski, and M. Neilan. Recent developments in numerical methods for fully nonlinear second order partial differential equations. *SIAM Review*, 55(2):205–267, 2013.
8. X. Feng and Th. Lewis. Nonstandard local discontinuous Galerkin methods for fully nonlinear second order elliptic and parabolic equations in high dimensions. *J. Sci. Comp.*, 77(3):1534–1565, Dec 2018.
9. R. Glowinski, H. Liu, S. Leung, and J. Qian. A finite element/operator-splitting method for the numerical solution of the two dimensional elliptic Monge-Ampère equation. *J. Sci. Comp.*, 79:1–47, 2018.
10. G. Loeper and F. Rapetti. Numerical solution of the Monge-Ampère equation by a Newton's algorithm. *C. R. Math. Acad. Sci. Paris*, 340(4):319–324, 2005.
11. M. Picasso, F. Alauzet, H. Borouchaki, and P.-L. George. A numerical study of some Hessian recovery techniques on isotropic and anisotropic meshes. *SIAM J. Sci. Comp.*, 33(3):1058–1076, 2011.
12. S. Stojanovic. Optimal momentum hedging via Monge-Ampère PDEs and a new paradigm for pricing options. *SIAM J. Control and Optimization*, 43:1151–1173, 2004.